The Shock Tube as a Short Duration Wind Tunnel

AUTHOR(S):

KAMIMOTO, Gorō; SHIMIZU, Takashi; AKAMATSU, Teruaki

CITATION:

KAMIMOTO, Gorō ...[et al]. The Shock Tube as a Short Duration Wind Tunnel. Memoirs of the Faculty of Engineering, Kyoto University 1958, 20(3): 163-181

ISSUE DATE:

1958-08-15

URL:

http://hdl.handle.net/2433/280414

The Shock Tube as a Short Duration Wind Tunnel

By

Gorō KAMIMOTO, Takashi SHIMIZU and Teruaki AKAMATSU

Department of Mechanical Engineering

(Received April 30, 1958)

Abstract

Descriptions of the shock tube recently constructed at Aerodynamic Laboratory and of some experimental results obtained thereby are given in this paper.

The shock tube has a cross section of 156 mm high and 50 mm wide and is 3370 mm long. By this shock tube a uniform flow field, free from turbulence, is obtained and its Mach number may freely be adjusted from zero to the supersonic range.

Instantaneous photographs of the flow patterns have been taken by using the Mach-Zehnder interferometer or the schlieren method and are shown in this paper.

1. Introduction

In recent years, the shock tube is being used in experimental studies of the subsonic, supersonic and hypersonic aerodynamics, the growth of unsteady boundary layer and the detonation, etc.

What is called "the Shock Tube" consists of a constant-area duct separated by a thin diaphragm into the regions of high and low pressure. When the diaphragm is raptured, the disturbances are propagated in both directions; a rarefaction into the high pressure chamber and a compression in the low pressure channel, and in the latter a shock developes. Behind this shock, a uniform quasi-steady flow is attained and it becomes either subsonic or supersonic flow depending upon the initial pressure ratio across the diaphragm.

Since the interval of this flow is extremely short, in the order of one millisecond, it is necessary to use special electronic and optical equipments. But this shock tube is an economical one as a research equipment for modern aerodynamics because of its low cost of construction and maintenance. From this point of view, we constructed in our laboratory a shock tube as a short duration wind tunnel.

2. The Operation and Theory of the Shock Tube

The conventional shock tube consists of a straight tube of uniform cross section

separated into the high and low pressure sections by a thin diaphragm. (We use cellophane as the diaphragm.)

Suppose that the gases in the low and high pressure sections are initially at the same temperature and the diaphragm is suddenly ruptured. A shock wave is generated and propagates through the low pressure gas, accelerating the gas and simultaneously raising the temperature on the low pressure compartment. The gas between the contact surface (which separates the gas in high pressure section and the gas in low pressure section) and the shock is at a uniform temperature and velocity. On the other hand, in the high pressure section, the gas expands as a rarefaction wave, whose front travels with the local velocity of sound of the high pressure gas. But the gas particles move to the same direction as the gas flow behind of the shock wave. This pattern is shown schematically in Fig. 1. After the first running of the waves, these shock wave and rarefaction wave reflect and a complicated wave pattern developes.

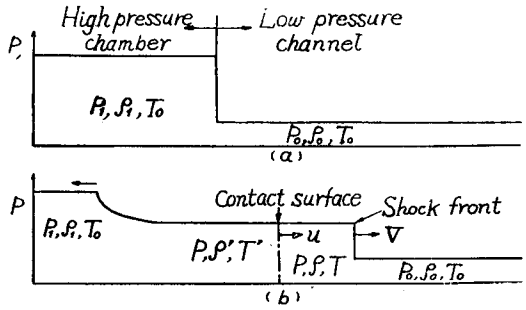

Fig. 1.

Let the original pressure in the high and low sections be denoted by p_1 and p_0, and the initial temperatures be equally given by T_0. A normal shock wave moves into the low pressure channel with the uniform supersonic velocity V. The gas particles in the low and high pressure compartments behind the shock acquire a uniform velocity u ($<V$), moving in the same direction as the shock. Since the gas behind the shock is compressed, its temperature T is higher than T_0; and since the gas behind the rarefaction wave is expanded, its temperature T' is lower than T_0. Consequently, a discontinuity of temperature occurs at the contact surface. Hence, the Mach number M of the flow between the shock and the contact surface becomes different from the Mach number M' of the flow between the contact surface and the expansion wave.

We can calculate theoretically the gas motion behind the shock wave[1,2]. Since the conventional shock tube uses air as its working fluid, we assume that its specific heat ratio γ is 1.40. The initial pressure ratio p_0/p_1 before and behind the diaphragm, the Mach number M and M' of the quasi-steady flow behind the shock and the contact surface respectively, and the strength of shock p/p_0 are as follows:

$$\frac{p_0}{p_1} = 6\left[7M_s^2-1\right]^{-1}\left[1-\frac{1}{6}\left(M_s-\frac{1}{M_s}\right)\right]^7 \qquad (1)$$

$$M = 5[M_s^2-1][(7M_s^2-1)(M_s^2+5)]^{-\frac{1}{2}} \qquad (2)$$

$$M' = 5[M_s^2-1][M_s^2+6M_s-1]^{-1} \tag{3}$$

$$\frac{p}{p_0} = \frac{1}{6}[7M_s^2-1] \tag{4}$$

where M_s is called the shock Mach number, $M_s = V/a_0$, and a_0 is the speed of sound in the initial low pressure gas.

Thus, if the initial temperature of the low pressure gas T_0 and the shock speed V are measured, other quantities, namely M, M' and p/p_0 can be theoretically determined from Eq. (2) to Eq. (4).

For the strong shocks ($p_0/p_1 \to 0$), the Mach number M of the flow between the shock and the contact surface approaches a limiting value and becomes 1.89, when the specific heat ratio of air is assumed to be $\gamma = 1.40$; while in the flow between the contact surface and the rarefaction wave the Mach number M' increases without limit. (assuming $\gamma = \text{const.}$) However, in reality, both the Mach number M and M' approach their respective limit values and their values are approximately[1,3] $M=3$ and $M'=4.5$. Nevertheless, the high supersonic flow can be easily obtained if the flow behind the contact surface is utilized.

The values of M and M' coresponding to the shock Mach number M_s are plotted in Fig. 2. The relation between M and p_0/p_1 can be found from Eqs. (1) and (2), which is shown by the solid curve in Fig. 3. Fig. 3 explains that a flow of desired Mach number can be obtained by variing the initial pressure ratio p_0/p_1. The points

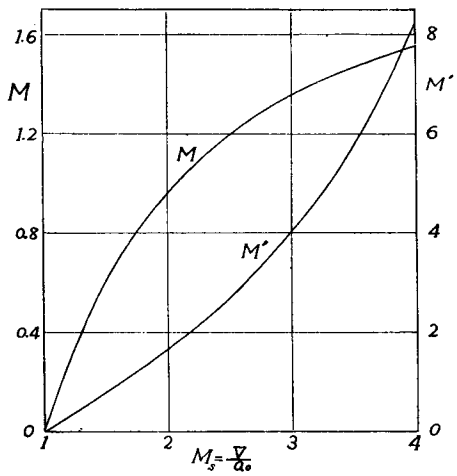

Fig. 2.

in Fig. 3 are the flow Mach numbers M observed by measuring electronically the shock speed V. (The method of measurement of the shock speed will be described below.) The observed Mach number M is a little less than that which is expected of the simple theory. This disagreement may be attributable to the effect of viscosity of air and the fact that the diaphragm does not burst in an ideal manner.

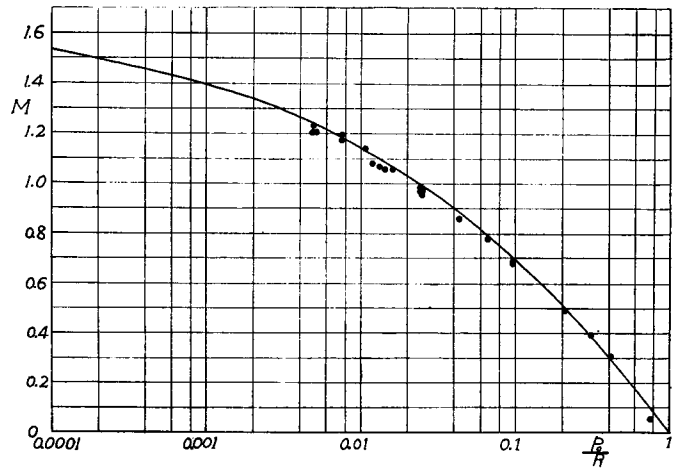

Fig. 3.

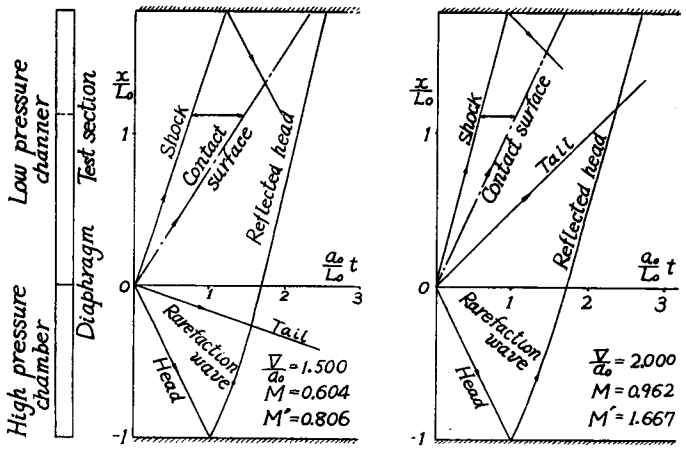

Fig. 4.

To explain the various effects which take place in the shock tube, the time -distance diagrams are drawn in Fig. 4 for the case of the particular shock Mach numbers of $M_s = 1.5$ and 2.0. The ordinates are in terms of the ratio x/L_0 of the distance x of the considered point from the diaphragm to the length L_0 of the high pressure chamber, while the abscissae are given by $a_0 t/L_0$, where t is time. The computations are performed, using the relations described above and others. The time required for the shock and the contact surface to reach the test section after the shock passes the 2nd. light screen (see Fig. 6) is shown in Fig. 5 as the function of Mach number M of the flow behind the shock. It is assumed here that the initial air temperature is 10°C.

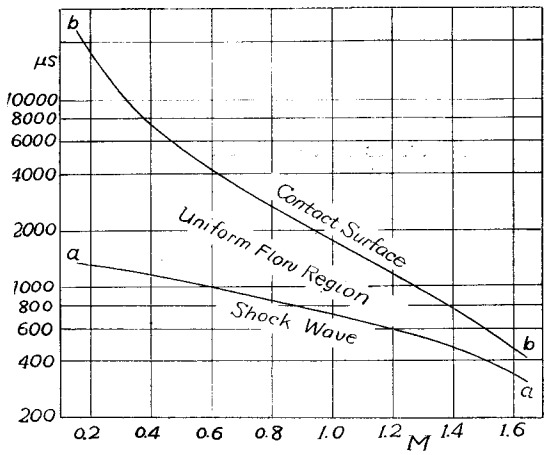
b
μs
10000
8000
6000
4000
2000
a
1000
800
600
400
200
Contact Surface
Uniform Flow Region
Shock Wave
b
a
0.2
0.4
0.6
0.8
1.0
1.2
M
1.4
1.6

Fig. 5.

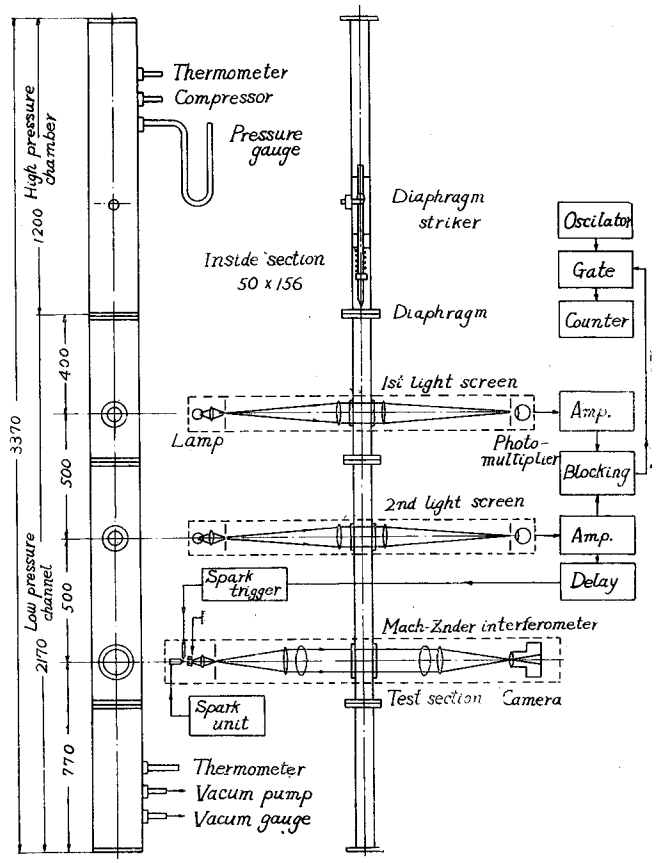
Thermometer
Compressor
Pressure gauge
High pressure chamber
1200
Diaphragm striker
Inside section 50 x 156
Diaphragm
Oscilator
Gate
Counter
1st light screen
Amp.
Lamp
Photo-multiplier
Blocking
2nd light screen
Amp.
Delay
Spark trigger
Mach-Zender interferometer
Test section
Camera
Spark unit
Thermometer
Vacum pump
Vacum gauge
3370
400
500
500
770
2170
Low pressure channel

Fig. 6.

3. The Construction of a Shock Tube Installation

A schematic diagram of overall shock tube installation and a photograph thereof are shown in Fig. 6 and Plate 1. A detailed description of the installation; i.e. the shock tube proper and the electronic and optical equipments, is as follows:

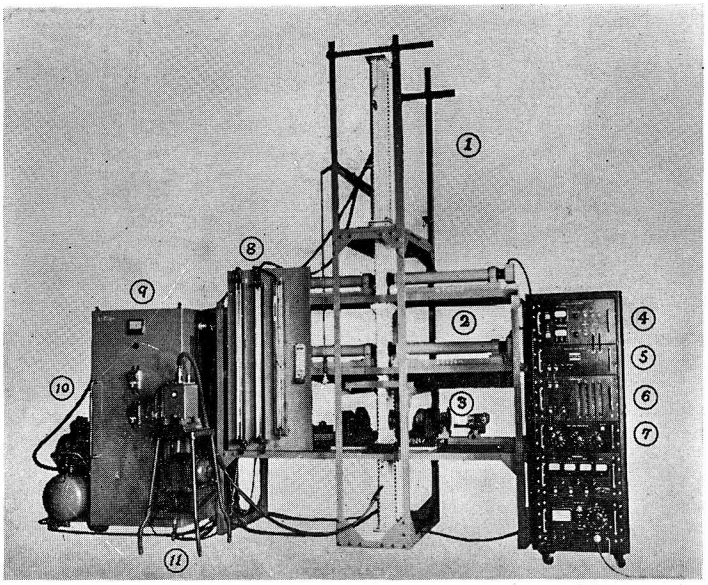

① Shock tube proper
② Schlieren light screen
③ Mach-Zehnder interferometer
④ Blocking unit
⑤ Gate unit
⑥ Counter unit
⑦ Time delay unit
⑧ Pressure gauge
⑨ High voltage unit
⑩ Compressor
⑪ Vacuum pump

Plate 1. Shock tube installation.

3.1. The Shock Tube Proper

3.1.1. Design Consideration

In designing a shock tube, the lengths of the two sections must be chosen to obtain a desired duration of the uniform flow, and the cross section must be also uniform throughout the length of the tube. In addition, the positions of the light screens and the working section along the tube should be properly apart from the diaphragm. The reason for it is that the more are these positions apart from the diaphragm, the more discontinuous becomes the shock front and the more uniform the flow behind it. Also, it is reported[1] that, in the case of a shock tube having a circular cross section, a well-formed shock is found at a distance of a few diameters

away from the diaphragm and that it is desirable to make observations at a distance 10 to 20 times the greatest dimension of the cross section from the diaphragm. To simplify the optical technique, it is desirable that the shock tube has a rectangular cross section, the width of which is sufficiently wide along the light path to give suitable optical effects. Thus the two-dimensional phenomena are observed. The longest possible length of the shock tube is preferable for the purpose of lengthening the flow duration and it is desirable to be able to vary its length.

Now, as the first trial, the tube of vertical type was constructed. Because of its vertical type, it was not neccesary to sweep up the shattered diaphragm every time the diaphragm was raptured, and mounting of the Mach-Zehnder interferometer was easily done. However, the overall length of the tube is often limited in this case because of its vertical type construction.

3. 1. 2. The Construction of the Shock Tube Proper

The tube is 50 mm×156 mm in cross section, 3370 mm long; the lengths of the high and low pressure sections are 1200 mm and 2170 mm respectively. (Fig. 6)

On the upper part of the high pressure chamber are mounted a high pressure air inlet pipe, a hollow to insert a thermometer and an outlet pipe attached to the pressure gage, and a diaphragm striker is mounted in the lower part of the chamber. This diaphragm striker has a sharp point and is operated by a spring. The spring is compressed and the striker is held in position by a distance piece until a cable pulls the distance piece off.

To facilitate the changing of diaphragms, the chamber is suspended from the frame work and its weight is balanced with the counter weight.

On the other hand, the low pressure channel is fixed on the frame work, and a vacuum gage and a outlet pipe leading to the vacuum pump are mounted on the lower part of the channel.

Two pairs of optical glass windows, 40 mm in diameter and 15 mm thick each, are fitted into the tube walls. The light beams of the miniature schlieren system traverse the tube through these windows, whose center line distance is 500 mm, at which distance the speed of the shock is measured.

At the working section, are fitted two optical glass plates of 80 mm diameter and 25 mm thick. The models are changed by taking these glass plates off.

The vacuum pump for evacuation of the channel is 1/2 H.P. in power, and the compressor supplying high pressure air to the chamber is 1 H.P. and its maximum pressure, 10 kg/cm^2. A chamber pressure is limited at present to about 2 kg/cm^2 gage by the static strength of the diaphragm and air leakage, and minimum channel pressure obtained is 3 mm Hg.

It is desirable that the pipe connecting the vacuum pump with the low pressure

channel is as large in inner diameter and as short in length as possible in order to attain a considerable quantity of vacuum. A rubber pipe of 15 mm inner diameter is used as a connecting pipe in this shock tube.

3. 2. The Electronic and Optical Equipments

The extremely short duration of the flow processes occurring in a shock tube necessitates the use of the electronic and optical equipments. Particularly, it is necessary to obtain the shock speed and to take instantaneously timed photographs of the flow patterns.

3. 2. 1. The Measurement of the Shock Speed

A schematic diagram of the measurement of shock wave velocity is given in Fig. 6. As the shock passes the 1st. schlieren system, the beam is momentarily deflected into the photocell. The pulse from the photocell, after modification, starts the electronic counter. The passage of the shock past the identical 2nd. schlieren system produces a pulse which stops the counter. Thus, the shock velocity is measured by noting the time of passage of the shock between the two schlieren light screens separated 500 mm apart as mentioned above.

(1) The Light Screens.

The detail of the schlieren light screen is given in Fig. 7. A and B are slits of 10 mm by 40 mm, and two pairs of the slits are spaced 500 mm interval along the tube axis. Light source L.S., condenser lens Lc, slit S, lenses L_1 and L_2, and knife edge K constitute a conventional schlieren system. The light beam, 10 mm wide and

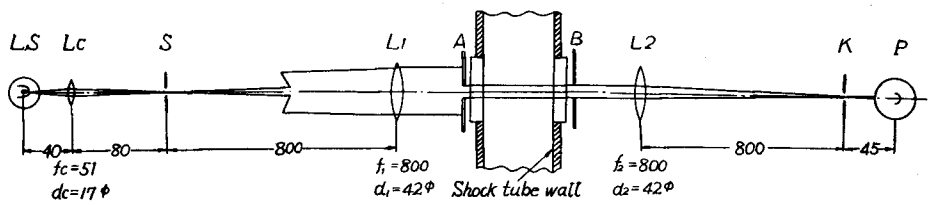

Fig. 7.

40 mm high, traverses the shock tube. When the shock passes the light screen, the beam is deflected beyond the knife edge K and falls on the photomultiplier tube P, which is shielded in a box. Thus, a signal is sent out.

The light screens are placed on the tables, which are mounted on the frame work detached from the shock tube proper in order to avoid mechanical vibrations. (Plate 1)

(2) The Photomultiplier and the Blocking Units

The detailed circuit diagrams of the photomultiplier and blocking units are given

in Fig. 8. The start and stop pulses from the photomultiplier tubes in the 1st. and 2nd. light screens are fed into the blocking unit, which consists of a bistable multivibrator, a gate tube and amplifiers, and feeds only the initial start and stop pulses to to the next gate unit, cutting off other pulses following them.

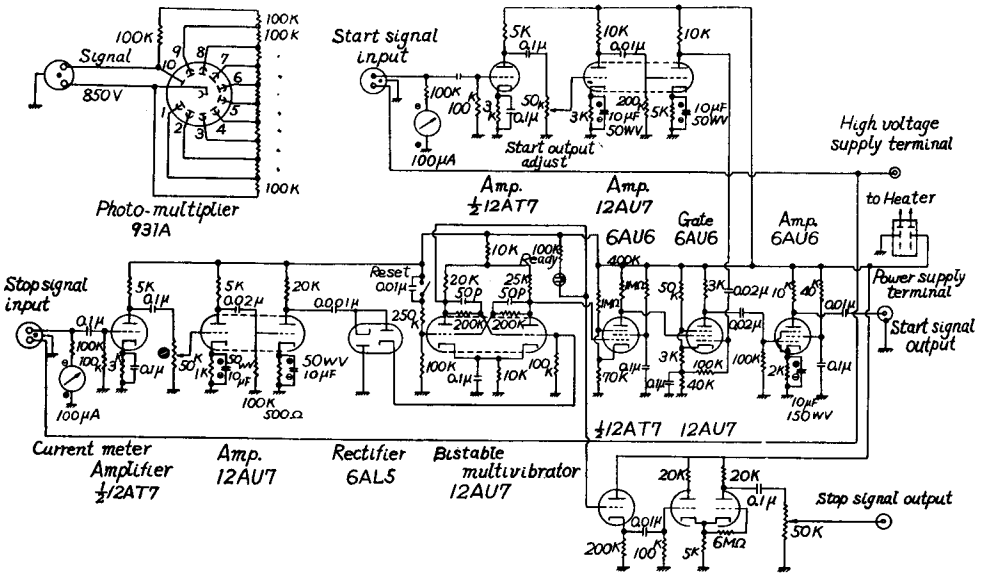

Fig. 8.

(3) The Gate and the Counter Units

To the blocking unit follow a crystal-controlled oscilator, an electronic gate and four decades. Since the frequency of the crystal oscilator is 250 kc/sec, one count corresponds to 4 microsec. and the counting range extends from 0 to 9999 counts.

The detailed circuits of a crystal controlled oscilator and an electronic gate are shown in Fig. 9, and the counter circuit in Fig. 10. Fig. 10 shows some main parts of the 1st. (×1) and 2nd. (×10) figures in the counter and the circuits similar to them are repeated in the 3rd. (×100) and the 4th. (×1000) figures.

Before experiment, the gate is kept shut. Receiving a start pulse from the blocking circuit, the gate is opened and the decades count the individual cycles (each 4 microsec.) coming from the oscilator. This process continues until a stop pulse shuts the gate, and the number of pulses coming from the oscilator is indicated by lighting of neon lamps on the counter and remains displayed until the reset button is pushed. The time interval between the start and stop pulses in terms of microsecond is four times the counter indication. Thus, the shock velocity is computed by dividing the distance of 500 mm between the two light screens by the time interval

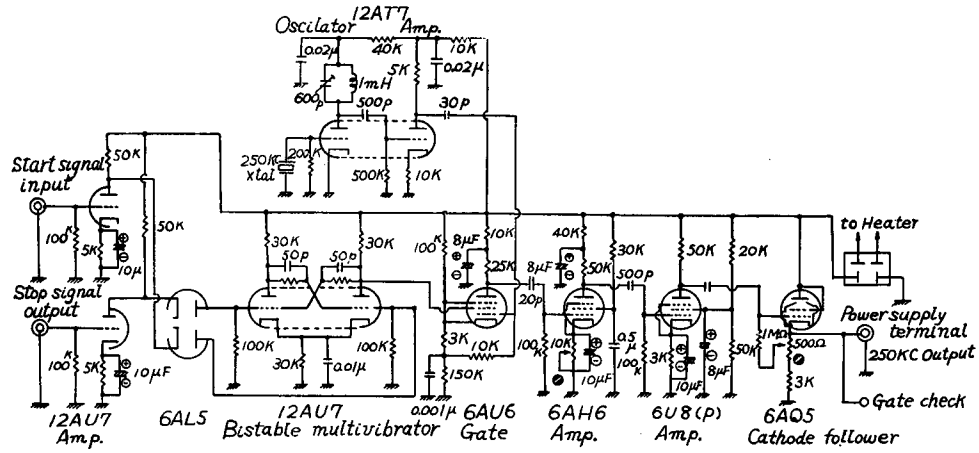

Fig. 9.

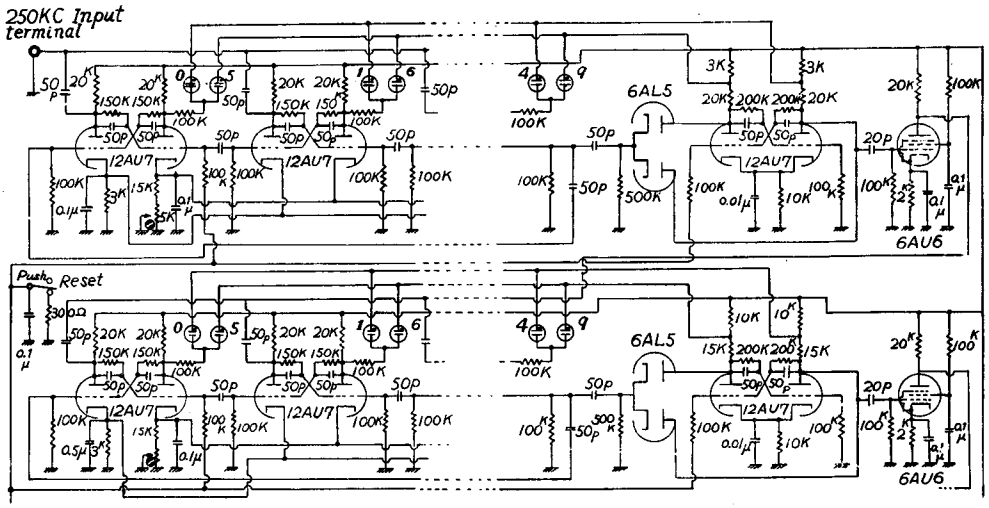

Fig. 10.

indicated by the counter. In the course of our investigation, the counter became unreliable and miscounting frequently occurred. This most likely have been caused by the fact that blocking unit is directly connected to the photomultiplier. Therefore, we intend to insert a preamplifier between them; then, we consider, good results can be obtained.

3. 2. 2. The Spark and the Time Delay Units

A spark gap is the effective light source, because it is small in size and has a short duration of the order of 1 microsecond or less. A high voltage is required to operate air spark gap efficiently.

The circuit diagrams of the spark unit and the high voltage unit are shown in Fig. 11 and 12.

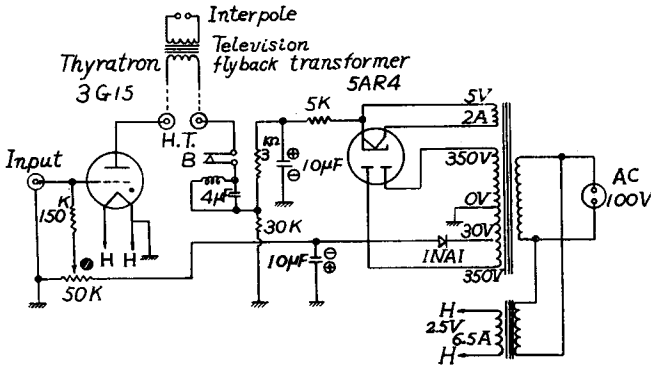

Fig. 11.

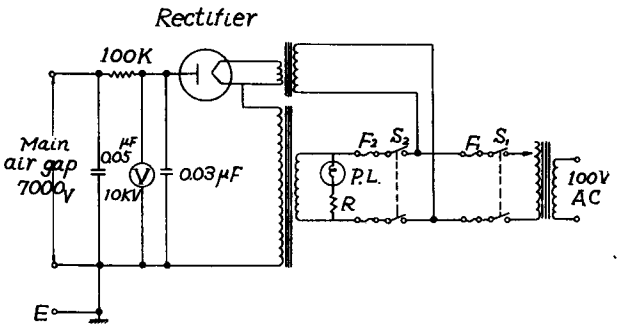

Fig. 12.

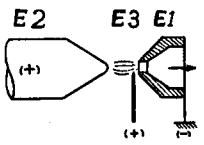

Fig. 13.

The spark gap consists of the two magnesium electrodes E1, E2 and the third electrode E3 as shown in Fig. 13. The light from the spark is taken out through a hole drilled in the 1st. electrode, thus providing a suitable point source for photography. The gap between the electrodes is about 5 mm and they are connected to the ground and the high voltage, which is charged to a condensor of 0.05 microfarad through a diode and a transformer. The 3rd. electrode is inserted in the spark gap close to the hole and it triggers the spark. The pulse coming from the 2nd. light screen actuates on adjustable electronic delay circuit. Fig. 14 is a circuit diagram of the time delay unit, which is composed of the monostable multivibrator, the pulse sharpener and the cathode follower. The delay time depends on the capacity of the timing switch shown in Fig. 15. These circuits have delays of 200 to 2620 microsecond. The final pulse output from the time delay

unit triggers the light source so that a photograph of the flow can be taken at any predetermined instant. (see Fig. 5)

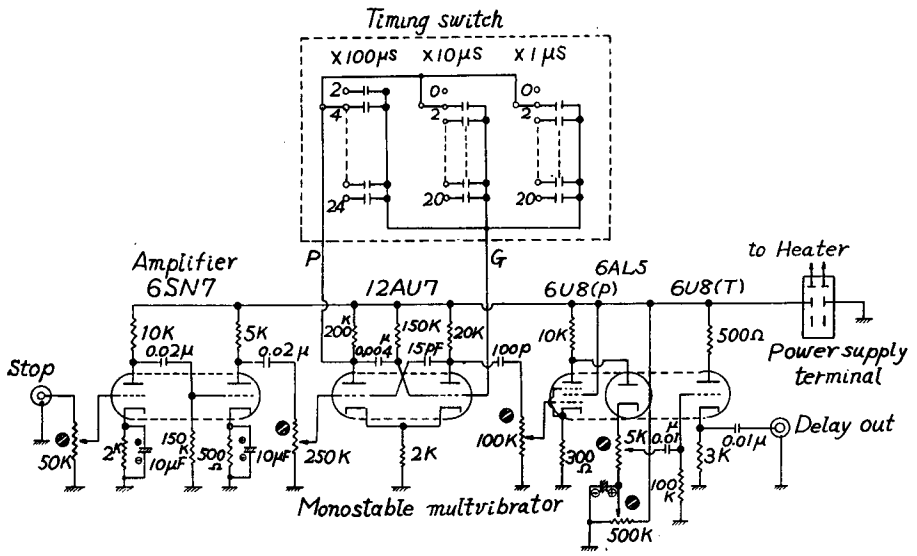

Fig. 14.

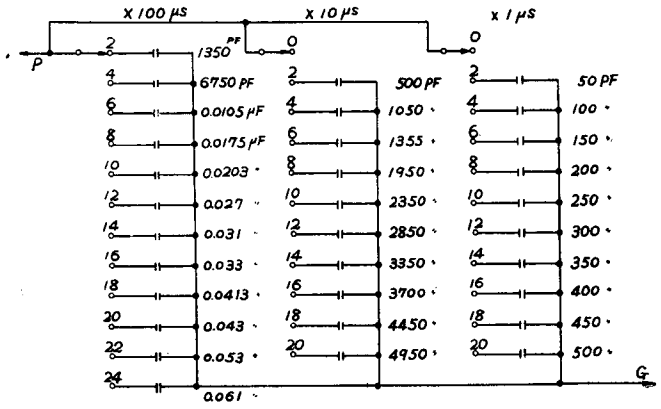

Fig. 15.

The thyratron is fired by the output pulse from the time delay circuit and a discharge takes place, by which an instantaneous high tension is induced at the 3rd. electrode through an induction coil. (This coil is a fly back transformer for television.) Thus, the trigger gap between the 1st. and 3rd. electrodes breaks down and a spark is induced in the main air gap.

In the spark units, the resistance and inductance of the circuits should be decreased

so as to minimize the duration of the discharge. Also, in order to reduce delay of the spark, it is desirable to maintain the high tension on the two electrodes in a critical condition so that the main discharge is induced by a slight impulse of the preliminary spark. However, the critical tension in the spark gap fluctuates in accordance with the conditions of the atomosphere and the surface conditions of the electrodes. The fluctuation of the total delay time, which is the time required from the passage of the shock through the 2nd. light screen to the discharge taking place in the main gap, occasionally reached about one hundred microsec. Therefore, we are considering of reducing this fluctuation as much as possible.

3. 2. 3. Mach-Zehnder Interferometer

The flow pattern can be observed by an interferometer, which allows the quantitative measurements of density and the subsequent calculation of the temperature, pressure and velocity in a flowing gas. Fig. 16 is a schematic diagram of the interferometer and the associated optical equipments. Light from the source L.S. is passed through a filter F and focused by a lens L_0 on a slit S, and this slit is also at the focus of a lens L1 which makes the light parallel. This parallel beam is divided by the beam-

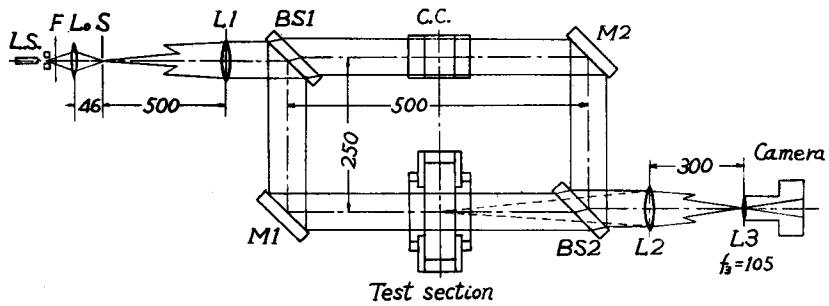

Fig. 16.

splitter BS1, the reflected beam proceeds to the plane mirror M1 and pass through the test section; and the transmitted beam proceeds on the plane mirror M2 passing through the compensator. These two beams are recombined by the beam-splitter BS2. These beams are coherent and produce interference fringes, which are then focused on the screen of the camera by the lenses L2 and L3.

By the way, if the knife edge is placed at the focus of lens L2 and the beam transmitted from BS1 is cut off, and only the beam reflected by BS1 is passed through the test section, this instrument becomes a schlieren system. Now, if the both beams are passed, a system combining the interferometer with the schlieren method is set up. These four plates are 105 mm diameter; however, being inclined 45° to the optical axis, their effective diameter is 60 mm. These beam-splitters and the glass

plates of the window in the test section and the compensation chamber possess high quality optical flats and uniform optical thickness such as are required for interferometer and the mirrors also have high quality optical flats. These plates are coated to prevent further loss of light. Especially, the coating of the beam-splitters and mirrors are nonmetallic and very efficient for a restricted wave length region (4481 Å). The two beam-spliters can be rotated around a horizontal and a vertical axis, and a pure translation alone is also possible. The other two mirrors are also provided with combined mechanisums of translation and rotation.

The dimensions of the rectangular path of light shown in Fig. 16 are so selected that M1 is twice as far as the distance between M2 and BS2. Since the test plane is located midway between M1 and BS2 such that the optical paths from M2 and from the test plane to the observation screen are equal, the fringe pattern can be adjusted by M2 without being out of focus[4]. The four plates are adjusted parallel to each other with the aid of an autocollimeter, a penta-prism and mercury level. Further, they can also be adjusted by a method of placing cross hairs before BS1[5]. Each of these plates are mounted on an optical bench which is set on a table. This table is detached from the shock tube proper so that mechanical vibration in the tube will not disturb the optical system.

The conventional method of identifying the fringes across the discontinous shock is generally done by use of white light fringes. However, when a white light source was used in, a few central fringes appeared clearly if the glass windows in the test section and in the compensation chamber were removed from the interferometer system; and if they were fitted up, about ten each of the blue and the red fringes appeared and the central fringes became obscure. This might have been due to the fact that the surfaces of the glass plates were not perfectly parallel. Therefore, for the purpose of tracing the fringes through the shock, we must adopt another technique: the so-called off-set method of light axis.

As a light source, a spark between magnesium electrodes was used, and the strongest spectral line (4481 Å) was selected by a gelatin filter K6.

4. Experimental Procedure and Results

4.1. Operational Procedure

A brief résumé of procedure of the operation is as follows:

(1) Bring the camera into focus on the plane distant one-third of the test section width inward from the exit window[4], and make parallel fringes having desired numbers and direction on the screen by adjusting the beam-splitters.

(2) Switch on the electronic equipment and wait until the warming up period—about twenty minutes in our equipment—has elapsed. Check the operation of the

counter by using a pulse generator, by which start and stop pulses at the interval 50 microsecond, 100 microsecond and 500 microsecond are generated intermittently.

(3) Let multiplier current be 5 microampere by adjusting the knife edge position of the light screens so that each multiplier tube will detect even a slight change of illumination.

(4) Keep the high tension on the spark gap at a critical conditions.

(5) Fit a diaphragm to the shock tube and clamp the chamber to the channel. Switch on the vacuum pump and allow the channel pressure to reach the desired value. Then, allow high pressure air to enter the chamber until the pressure reaches a desired value, or the chamber may be left at the atmospheric pressure.

(6) Record the pressures of both sections and of the atmosphere, and also note the air temperature.

(7) Referring to Fig. 5, decide the delay time from the time the shock passes through the 2nd. light screen until it triggers the spark, and tune the delay timing switch.

(8) Expose the film for a short interval, including the instant when the diaphragm is raptured by pulling a cable. Thus, a timed photograph is taken.

4. 2. Experimental Results

The timed photographs of the shock waves over a cylinder and a wedge, and of the high subsonic flow around the wing sections were obtained by using the interferometer or the schlieren method. Typical photographs of these are shown in Plate 2, 3, 4, 5, 6 and 7.

For the sake of simplicity, let the gas flow behind the shock and the contact surface be called the 'hot' gas and the 'cold' gas respectively.

First, a set of experiments were made to determine the location and shape of the

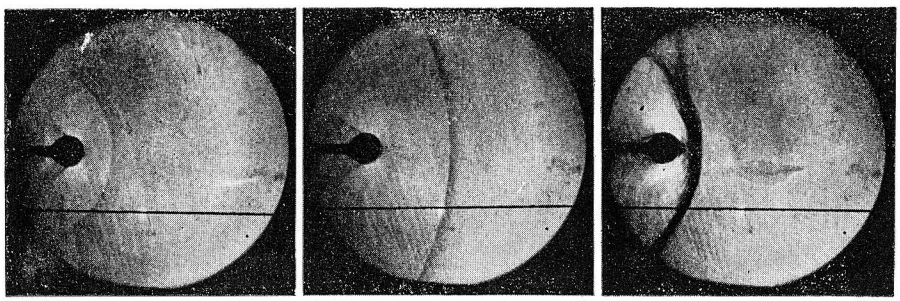

(a) M=1.10 D.T.=600μs (hot gas)

(b) M=1.10 D.T.=700μs (hot gas)

(c) M′=2.2 D.T.=900μs (cold gas)

Plate 2. Schlieren Photographs (cylinder)

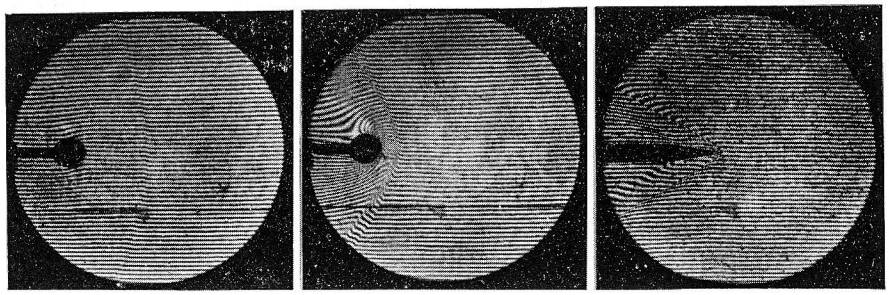

(a)
M=1.15 D.T.=600μs
(hot gas)

(b)
M′=2.40 D.T.=1300μ4
(cold gas)

Plate 3. Interferograms (cylinder)

M′=2.40 D.T.=1300μs
(cold gas)

Plate 4. Interferogram (20° wedge)

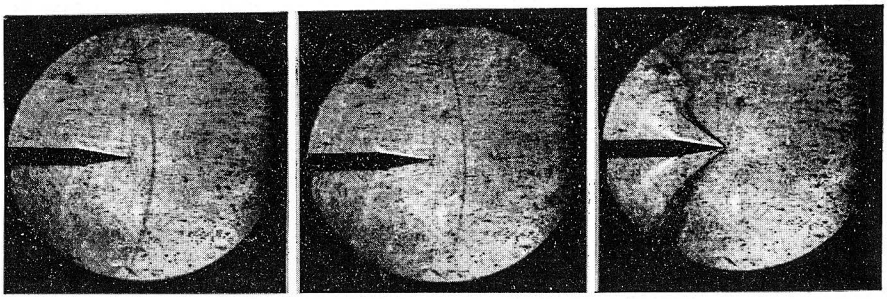

(a)
M=1.13 D.T.=600μs
(hot gas)

(b)
M=1.13 D.T.=900μs
(hot gas)

(c)
M′=2.25 D.T.=1200μs
(cold gas)

Plate 5. Schlieren photographs (20° wedge)

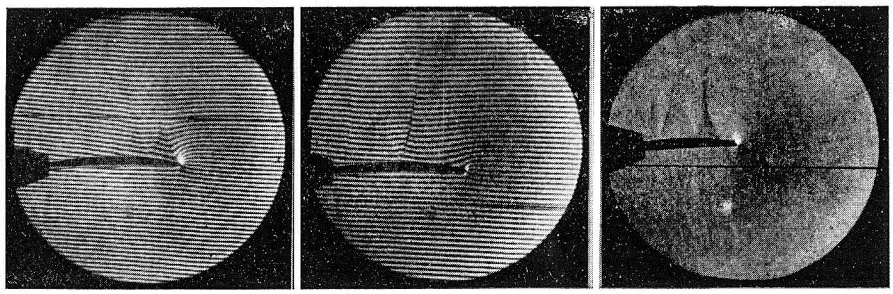

(a)
M=0.65 D.T.=1500μs
incidence angle α=3.7°

(b)
M=0.725 D.T.=700μs
α=3.7°

Plate 6. Combined schlieren-interferograms

M=0.725 D.T.=900μs
α=6.1°

Plate 7. Schlieren photograph

detached bow wave on a cylinder and a wedge in the 'hot' gas flow of Mach number 1.05, 1.10, 1.15, 1.20 and 1.25. For each Mach number, timed photographs were taken at the various delay time at which the spark is triggered. Now, as the counter became unreliable, the flow Mach number was determined from only the initial pressure ratio. The pressure of the chamber was kept at the atmospheric conditions throughout these experiments.

The cylinder was 6.5 mm in diameter, and the wedge was 3.5 mm thick and 20° total angle. These models were clamped between the walls of the working section by spring force of their supporting arms.

In Plate 2 are shown schlieren photographs of the flow around the cylinder: (a) and (b) are the photographs of the 'hot' gas flow and show the developments until a steady state was reached, and (c) is that of the 'cold' gas flow. The Mach number and delay time are shown simultaneously. In Plate 3 are given the interferograms of the same cylinder. The fringe shift in 'hot' gas flow was very little: about 1/4 fringe even at the discontinuity, such as, of the shock wave. Therefore, it was impossible to measure the density distribution over the entire field. For this reason, it is necessary to obtain a larger fringe shift by increasing the initial pressure. However, the fringe shift across the bow wave agrees considerably with the theoretical value.

Photographs of the wedge also are shown in Plate 4 and 5. In the 'cold' gas region, the shock wave already attaches the wedge due to higher Mach number. These schlieren photographs are quite dirty. They were soiled by the grease which was used for air-tightening at the joints and they scattered at every operation of the shock tube. Therefore, it is desirable not to use grease at all, if possible. Judging from these photographs, it proves the fact that the 'hot' and the 'cold' gas flows are uniform and not turbulent except the mixing region at the contact surface.

Next, let us show the bow wave distance as a function of Mach number. Fig. 17 shows the case of the cylinder. The solid line is the curve calculated by Moeckel's method[6]. The points are the experimental values. A set of points plotted vertically show the location of the bow wave

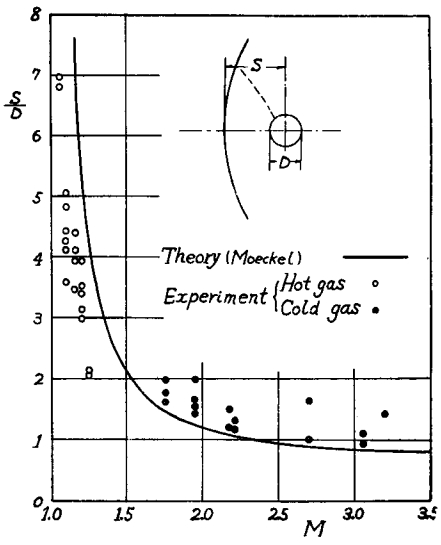

Fig. 17.

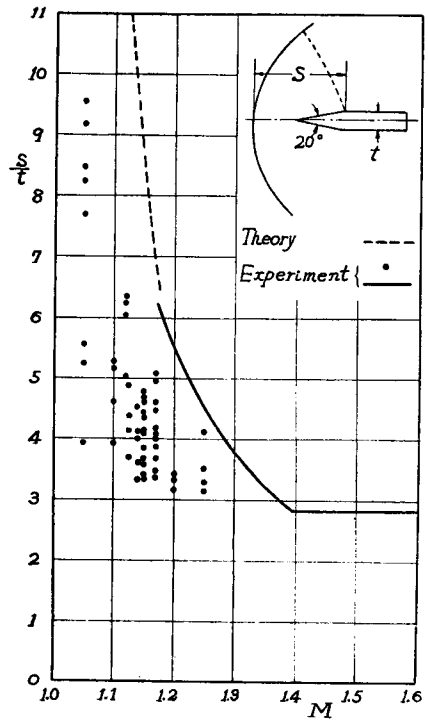

Fig. 18.

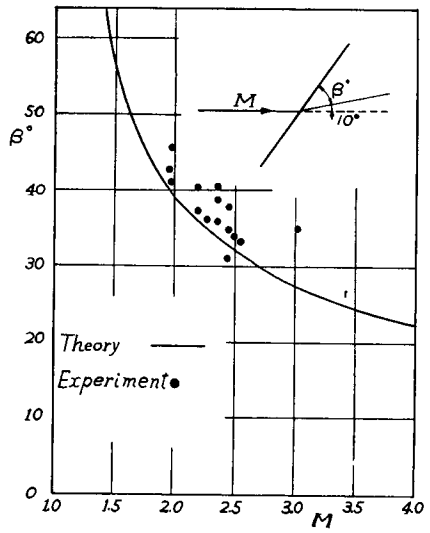

Fig. 19.

at various time for the same Mach number flow. In the 'hot' gas flow, the experimental results are below the theoretical values. This means that the bow wave has not yet reached the steady state.

Fig. 18 is the case of the wedge in the 'hot' gas flow. The dashed and solid lines are the theoretical and experimental curves respectively shown in Ref. 7. The shock wave inclination which developes on the wedge in the 'cold' gas flow is shown in Fig. 19 as a function of the Mach number determined from the initial pressure ratio. The solid line is the curve obtained from the oblique shock theory.

After the electronic circuits being more reliably operated, we can investigate in detail the process up to the point where the bow wave reaches an equilibrium position of steady flow.

In Plate 6 are given the photographs of high subsonic flow around a wing section: (a) and (b) are the combined schlieren-interferograms. In Plate 7 is also given a schlieren photograph of the flow around another wing section. Since the Reynolds number is low (about 10^5), the lambda shock waves appear on the upper surface.

5. Conclusion

A survey of the shock tube theory, the construction of a shock tube installation and of the experimental results obtained by it has been described.

As an application of the shock tube to study unsteady flows, timed photographs of the bow wave over a cylinder and a wedge approaching a steady state were obtained

by using the Mach-Zehnder interferometer and the schlieren method.

The shock tube will be applied more and more to the high temperature research at hypersonic flow and the study of unsteady flow. Having vast fields of application and its expenditure being low, the shock tube, even the small type units, will be very valuable for general research works.

Acknowledgements

The optical equipments of this installation, namely, Mach-Zehnder interferometer and light screens, were made by Shimadzu Seisakusho, Ltd.; and the electronical equipments, i.e. the counter, delay and spark trigger units, by Nippon Denkikizai, Ltd.

The authors wish to express their hearty appreciation to Mr. H. Ozawa and Mr. K. Ōsawa of the companies mentioned above, and to Mr. M. Teraoka who developed, printed and enlarged the photographs, and also to Mr. S. Ninomiya for his assistance in conducting the experiments.

References

1) Walker Bleakney, D. K. Weimer and C. H. Fletcher: The Shock Tube: A Facility for Investigations in Fluid Dynamics. Rev. Sci. Inst. vol. 20 (1949).
2) B. D. Henshall: On some Aspect of the Use of Shock Tubes in Aerodynamic Research. R. & M. No. 3044 (1955).
3) A. Hartzberg: The Application of the Shock Tubes to the Study of the Problems of Hypersonic Flight. Jet Propulsion, vol. 26, No. 7 (1956).
4) High Speed Aerodynamics and Jet Propulsion. vol. IX Physical Measurements in Gas Dynamics and Combustion. Princeton Univ. Press, P. 52 (1954).
5) John Winckler: The Mach Interferometer Applied to Studying an Axially Symmetric Supersonic Air Jet. Rev. Sci. Inst. vol. 19, No. 5 (1948).
6) Ascher H. Shapiro: The Dynamics and Thermodynamics of Compressible Fluid Flow, P. 884 (1953).
7) Wayland Griffith: Shock Tube Studies of Transonic Flow over Wedge Profile, J. Aero. Sci. vol. 19, No. 4 (1952).
The following publications benefited the authors throughout the present work.
8) H. W. Liepmann and A. E. Bryson, JR.: Transonic Flow Past Wedge Section, J. Aero. Sci. vol. 17, No. 12 (1950).
9) Harry T. Ashkenas, Arthur E. Bryson: Design and Performance of a Simple Interferometer for Wind-Tunnel Measurement, J. Aero. Sci. vol. 18 (1951).
10) Ryūma Kawamura and Haruo Saito: The 5×15 cm Shock Tube at I. S. T., Tokyo Univ. Report of I. S. T. vol. 9, No. 4 (1955).
11) Fumio Tamaki: The Shock Tube, Tokyo Univ. Report of I. I. S., vol. 4, No. 3 (1954).
12) Fumio Tamaki: The Instantaneous Photograph in High Speed Aerodynamics, Tokyo Univ. Report of I. I. S., vol. 6, No. 3 (1953).